doi:10.1016/j.ijrobp.2009.01.034

PHYSICS CONTRIBUTION

EVALUATION OF LINEAR ACCELERATOR GATING WITH REAL-TIME ELECTROMAGNETIC TRACKING

RYAN L. SMITH, B.S.,* KRISTEN LECHLEITER, M.S.,* KATHLEEN MALINOWSKI, M.S.,*
D. M. SHEPARD, PH.D.,† D. J. HOUSLEY, B.S.,† M. AFGHAN, PH.D.,† JEFF NEWELL, M.S.,‡
JAY PETERSEN, B.S.,‡ BRIAN SARGENT, B.S.,‡ AND PARAG PARIKH, M.D.*

*Washington University School of Medicine, St. Louis, MO; †Swedish Cancer Institute, Seattle, WA; and ‡Calypso Medical Technologies, Seattle, WA

Purpose: Intrafraction organ motion can produce dosimetric errors in radiotherapy. Commonly, the linear accelerator is gated using real-time breathing phase obtained by way of external sensors. However, the external anatomy does not always correlate well with the internal position. We examined a beam gating technique using signals from implanted wireless transponders that provided real-time feedback on the tumor location without an imaging dose to the patient.

Methods and Materials: An interface was developed between Calypso Medical's four-dimensional electromagnetic tracking system and a Varian Trilogy linear accelerator. A film phantom was mounted on a motion platform programmed with lung motion trajectories. Deliveries were performed when the beam was gated according to the signal from the wireless transponders. The dosimetric advantages of beam gating and the system latencies were quantified.

Results: Beam gating using on internal position monitoring provided up to a twofold increase in the dose gradients. The percentage of points failing to be within ±10 cGy of the planned dose (maximal dose, ~200 cGy) was 3.4% for gating and 32.1% for no intervention in the presence of motion. The mean latencies between the transponder position and linear accelerator modulation were 75.0 ±12.7 ms for beam on and 65.1 ± 12.9 ms for beam off.

Conclusion: We have presented the results from a novel method for gating the linear accelerator using trackable wireless internal fiducial markers without the use of ionizing radiation for imaging. The latencies observed were suitable for gating using electromagnetic fiducial markers, which results in dosimetric improvements for irradiation in the presence of motion.   © 2009 Elsevier Inc.

Respiratory gating, Radiotherapy, Organ motion, Treatment delivery, Real-time tracking.

INTRODUCTION

The goal of radiotherapy is to maximize the absorbed dose to the target volume while minimizing the dose to the surrounding healthy tissue. Intrafraction motion resulting from respiration can cause the tumor to move considerably throughout treatment. The displacements associated with respiration can be up to 3 cm within the thorax (1). To account for this motion, radiation oncologists must incorporate substantial margins (typically 1 cm in the superoinferior direction and 0.5 cm for both the anteroposterior and the lateral directions) in the design of each planning target volume. This leads to large volumes of irradiated healthy tissue that can limit the total dose the patient can safely receive. This has led researchers to explore beam gating techniques with the goal of more accurate radiation delivery to tumors affected by respiratory motion.

Respiratory correlation has been used extensively in computed tomography and magnetic resonance imaging in an effort to reduce breathing-related image artifacts (2, 3). More recently, similar techniques have been used to localize the tumor and gate the linear accelerator (4–8). Conventional gating setups use a variety of techniques to measure breathing motion, including optically tracked external marker blocks, thermocouples, thermistors, strain gauges, and pneumotachographs (9). Current techniques rely on the use of external markers or sensors to determine the internal position of the target. Although a correlation exists between external markers and internal tumor position, for some patients, external marker trajectories do not serve as an adequate surrogate for internal tumor position (10).

Respiration induces considerable deformation within the thoracic cavity. As the diaphragm contracts, the internal

anatomy compresses and distends. Often the external anatomy exhibits a good correlation with the motion of the internal structures such as the diaphragm and/or lung tumors (5, 10). The external anatomy moves from respiration; however, studies have shown considerable differences between the external anatomy and internal motion. These differences can come in the form of correlated motion with a phase lag between the external and internal motion, or, less frequently, the motion might not exhibit any correlation. Margeras and Yorke (11) have reported up to a 0.5-s lag between the Varian RPM marker block position and the diaphragm position measured fluoroscopically. Koch *et al.* (12) found that the correlation was poor and unstable unless the external surrogate measuring the skin surface position was near the tumor. In a study by Berbeco *et al.* (13), lung tumor motion was measured using continuous fluoroscopy concurrently with measurement of external abdominal surface positions. The amount of residual tumor motion, defined as the amount of tumor motion during a respiratory gate determined from the movement of the external surrogate, showed large fluctuations (>300%) for both intra- and interfraction motion. The residual motion was found to be up to 8 mm in magnitude, which strongly suggested that external position monitoring cannot accurately reflect the internal position of a tumor in all cases. The periods in which the external and internal motion exhibit poor correlation are often transient; however, these transient periods could have dosimetric implications (14).

The lack of correlation between the internal and external positions has led investigators to examine alternative techniques for accurately tracking the position of targets inside the thoracic cavity. Shimizu *et al.* (15) developed a real-time target tracking system that uses four integrated kilovoltage imaging systems. The fluoroscopic imaging system used in this technique provides accurate information on the location of discrete points inside the abdomen. However, accurate tracking of the target comes at the expense of an increased imaging dose. For a single fluoroscope, the estimated skin surface dose rate can up be to 118 cGy/h (16). In addition, for three-dimensional (3D) target tracking, stereoscopic fluoroscopes are necessary, resulting in accumulated dose because of imaging.

The Synchrony Respiratory Tracking System treatment option of the CyberKnife robotic radiotherapy system provides another image-based system for tracking internal fiducial markers (17). With that technique, gold fiducial markers are placed inside the thoracic cavity near the tumor, and the patient wears a vest with light-emitting diodes that indicate the position of the chest or abdomen. Before the treatment begins, a series of orthogonal X-ray images are acquired that are used to correlate the position of the external markers to the internal fiducial markers. A correspondence model is developed, and periodic images are obtained during the course of delivery to ensure that the correspondence model remains valid. Although the Synchrony Respiratory Tracking System delivers a lower radiation dose to the patient compared with continuous fluoroscopic imaging, this is achieved at the

expense of intermittent absolute knowledge of the internal positions. The Task Group 75 guidelines state that the entrance dose per image can be as great as 0.2 cGy (18). For a 2-h session with imaging performed every 30 s, the patient would receive 48 cGy during the treatment course.

Alternative image-based solutions have been investigated that use the on-board imaging functionality of many modern linear accelerators (19). Similar to the fluoroscopy-based solutions, on-board imaging solutions deliver a dose to the patient to image and track the internal markers or tumors. Another factor limiting this technique is that, if used simultaneously, high-energy megavoltage scatter from the treatment beam can degrade the image quality of the kilovoltage images used for tracking (20). Imaging-based methods have the advantage of providing information about the surrounding tissue, something a pure electromagnetic position monitoring solution cannot provide.

Continuous electromagnetic position monitoring is now available without an additional dose to the patient (Calypso Medical, Seattle WA). The system uses one or more wireless transponders, which are subject to performance testing as a part of the manufacturing operation to ensure they can stand up to high radiation levels throughout the treatment process. The transponders are currently implanted into the prostate using a 14-gauge needle in a procedure similar to gold fiducial implants currently in use clinically. During treatment planning, the transponder locations, as indicated by volumetric imaging, are recorded with respect to the isocenter and a plan is developed. During delivery, an array is placed above the patient. Four source coils in the array excite the transponders by magnetic induction. After excitation, 32 receiver coils in the array detect the resulting response signal. Each transponder has a unique resonant frequency, and they are sequentially exited to independently query the 3D position information. The array is registered to the room using stereoscopic infrared cameras, and the transponder position is known with respect to isocenter. Balter *et al.* (21) have reported submillimeter accuracy when tracking the transponders moving at 3 cm/s in a volume 14 × 14 cm in width and ≤27 cm away from the array. An additional study by Santanam *et al.* (22) confirmed submillimeter accuracy using concurrent onboard kilovoltage imaging. In a clinical prostate cancer treatment study, Willoughby *et al.* (23) have shown the system to be functional in a linear accelerator environment, even when the linear accelerator is treating directly through the array. No failures of the transponders from the radiation dose have occurred. The system has been cleared by the Food and Drug Administration for use in the prostate and prostatic bed. Potential applications in the lung and abdomen (where motion is substantial) are promising.

In the present study, we investigated the feasibility of using real-time electromagnetic tracking for linear accelerator gating. The system uses a spatial gating technique that gates the beam by way of the absolute 3D position of the internal fiducial markers (Fig. 1) instead of using phase or amplitude like conventional external surrogate systems currently in use.
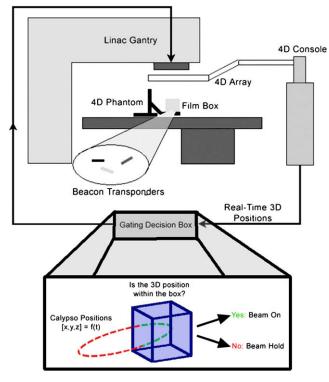
Fig. 1. Spatial gating setup. Four-dimensional phantom moves attached film phantom in realistic breathing trajectories. Real-time position information of transponders implanted in film phantom are acquired using array and sent to decision-making computer. Each position measurement is analyzed to determine whether it is inside a predefined three-dimensional volume. If so, the beam is turned on and delivery proceeds. If position is outside volume, beam hold is enacted and delivery halts until target returns.

This approach has two primary advantages. First, the beam is gated using the internal position of the tumor, thereby providing highly accurate positional information. Second, it does not require an additional imaging dose.

METHODS AND MATERIALS

The Calypso four-dimensional (4D) electromagnetic localization system was modified to export real-time position information to a spatial gating prototype. The prototype consisted of a personal computer that accepted the real-time information via Ethernet and a software application that controlled a transistor-transistor logic signal through the parallel port. The software compared the real-time 3D position information with a predetermined 3D volume to determine whether to enact a beam hold (Fig. 1). Issues surrounding the clinical determination of this 3D volume are addressed in the discussion section. The gating prototype would open and close an electrically isolated relay attached to the "beam hold" interface of a Varian linear accelerator (Varian Medical, Palo Alto, CA) in the same manner described by others (9). The transistor-transistor logic signal from the decision gating prototype was routed directly to the gating board, with plans to later incorporate a Varian-designed gating interface, which will provide additional buffering, isolation, redundancy, and safety checks. This transistor-transistor logic signal operates by opening a +12-volt signal, which goes to the timer interface board in the Clinac. This signal combines with other logic on the timer interface board and sets delayed electron gun triggers when the Clinac

is to be gated off. This causes the electron gun to be asynchronous to the RF pulse of the linear accelerator; thus, suppressing the beam. When the target is inside the 3D volume, the logic on the timer interface sets the gun triggers to be synchronous with the RF pulse of the Clinac, allowing a beam pulse to be delivered.

Gating: arc trajectories

Feasibility tests were performed to demonstrate linear accelerator gating using positional information from the Calypso system. A standard Calypso quality assurance phantom preloaded with three wireless transponders was placed on a rotating circular motion platform 6 cm from the center of rotation. The Calypso system was set to track one transponder with an update frequency of 30 Hz. The individual transponders are excited sequentially. To increase the frequency of spatial position information, a single transponder was used for this gating application. Single transponders do not provide rotational information. For other applications, multiple transponders could be used, and the target could be gated by way of the centroid (and/or rotation of the transponder plane); however, this would come at the expense of increased latency. In addition, Parikh *et al.* (24) have shown comparable RMS error when measuring a single transponder position vs. multiple transponders (0.2 mm vs. 0.45 mm), with superior latencies for a single transponder (100-ms integration time per transponder). Typically, the Calypso system operates with an integration time of approximately 80% of the update period. The clinical system therefore has a 100-ms update period (10 Hz) with an 80-ms integration time. For this phase of the study at 30 Hz, the integration time was approximately 26 ms.

A 2×2-cm field was used to irradiate the phantom on a Varian 23EX accelerator. A gating window was established, and when the beacon was outside this window, the treatment was halted. Although the motion was "circular," it was confined to a relatively short arc (2.8 cm). Over the width of the gating window (2 mm), the motion can be considered linear, given that the radius of the arc was 6 cm. The gating window was defined only along the direction of motion. Three film measurements were performed to establish proof of concept. First, a beam was delivered to the static phantom. Second, a nongated delivery was performed, where the disk was programmed to rotate back and forth at 1.2 cm/s over an arc covering 2.8 cm. Finally, a gated beam delivery was performed using the same motion parameters with a gating window of 2 mm. The gating was performed over the center of the arc, with the phantom moving at peak constant velocity. The gating window was positioned such that the phantom moved into and out of the window in both directions of motion along the arc trajectory, allowing for a beam hold on exiting the volume and re-establishment of the beam when the phantom re-entered the volume.

Latency estimates

To determine the latency of the system, the signal directly from the dynamic phantom was compared with the "target current" test-point signal from the linear accelerator using a logic analyzer. The target current is the current measured at the metal target of the linear accelerator's electron beam; hence, this signal is analogous to the presence or absence of the treatment beam. Using the target current instead of radiographic methods permits a more precise measurement of the latency using standard test equipment. It also facilitates acquisition of large numbers of beam transitions to accumulate a histogram of latencies. The Calypso system was set to monitor the positions at 30 Hz, with an update period of approximately 26 ms. Using this method, a histogram of latencies was generated for the motion from 200 circular motion cycles (Fig. 2). The latencies
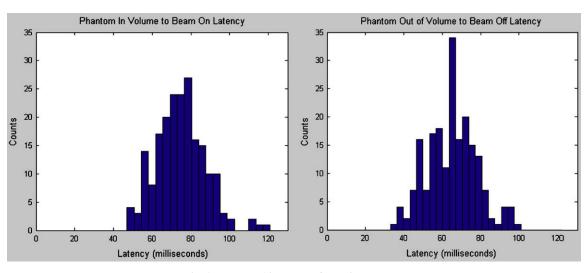
Fig. 2. Latency histograms for gating system.

were separated into two categories: beam-on latency and beam-off latency. Beam-on latency was defined as the duration from the target entering the gating volume (as indicated by a signal from the motion phantom) to the first observed target current pulse on the linear accelerator. Beam-off latency was defined as the duration from the target leaving the gating volume (as indicated by a signal from the motion phantom) to the last observed target current pulse on the linear accelerator.

Gating: clinical dosimetry

Clinically relevant dosimetric analyses were performed. A four-field, 6-MV, 200-cGy, 3D conformal radiotherapy plan for a random lung cancer patient was selected for this study. The treatment plan was developed using Pinnacle, version 7.1 (Philips, Madison, WI) and delivered using a Varian Trilogy linear accelerator. The phantom in the present study was composed of a standard solid water phantom with one sheet of the solid water replaced with an equivalently sized acrylic slab containing three electromagnetic transponders. The film phantom was attached to the Washington University 4D motion platform (25), which is a custom stage capable of reproducing physiologic tumor motion in all three axes to submillimeter accuracy. For each exposure, the film was placed in the coronal plane. The platform was programmed using respiratory motion data measured for a lung cancer patient using 4D-computed tomography and spirometry (26) (Fig. 3).

The gating system was operated using one transponder and a refresh rate of 25 Hz. The decision was made to use 25 Hz in this clinical dosimetry experiment instead of 30 Hz in the feasibility test because the greater sampling frequency is a difficult computation load for processing on a range of current-generation computing platforms. This should have a negligible effect on the latency, because the integration time only increased by 6 ms compared with 30 Hz. A gating window corresponding to exhalation (3-mm superoinferior margin) was used for lung delivery. The dose was delivered according to the following three scenarios: (*1*) to the static phantom, (*2*) to the phantom with the programmed motion patterns with no beam gating, and (*3*) to the moving phantom gated with signals from the Calypso system. The phantom motion was started simultaneously with the linear accelerator for each run. Analysis was performed to evaluate the dosimetric difference between the gated and nongated films compared with the reference static film irradiated in the absence of motion.

Radiographic film was used to record the dose (Kodak EDR2 Readypack, Rochester, NY) and was later digitized using a Vidar film scanner. During the experiment, an additional film was irradiated with a multileaf collimator plan that delivered a series of known doses. This film was digitized and used for Hurter and Driffield (H&D) curve calibration. This H&D curve was then used to calibrate the dose for the remaining films in the study.

RESULTS

Gating: arc trajectories

The film results from the initial phantom study showed a dramatic decrease in motion artifacts when comparing the dynamic gated and nongated films (Fig. 4). Because of the reduced motion artifacts, the dose for the dynamic gated delivery closely matched the dose delivered to the static phantom.
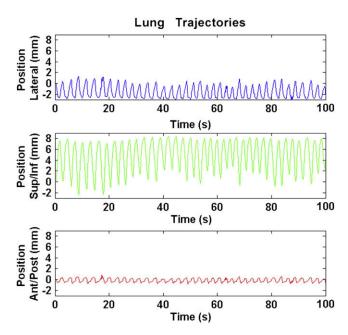

Fig. 3. Lung trajectories reconstructed from four-dimensional computed tomography and spirometry from a lung cancer patient (26).
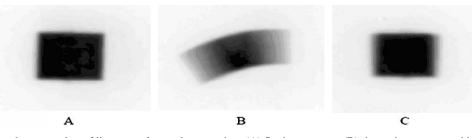
Fig. 4. Film demonstration of linear accelerator beam gating. (A) Static exposure, (B) dynamic exposure without gating, and (C) dynamic exposure with beam gating.

Latency estimates

The measurements showed that the latency was sufficiently small compared with the tumor velocity, thus providing high-quality dose localization. The mean latencies between the transponder position and linear accelerator modulation were 75.0 ± 12.7 ms for beam-on and 65.1 ± 12.9 ms

for beam-off, given as the mean $\pm$ standard deviation (Fig. 2). The difference between the beam-on and beam-off times could be attributed to asymmetry in the linear accelerator turn-on and turn-off times or partially to imperfect alignment of the phantom with respect to the Calypso gating volume. The range in the latencies can be attributed to the
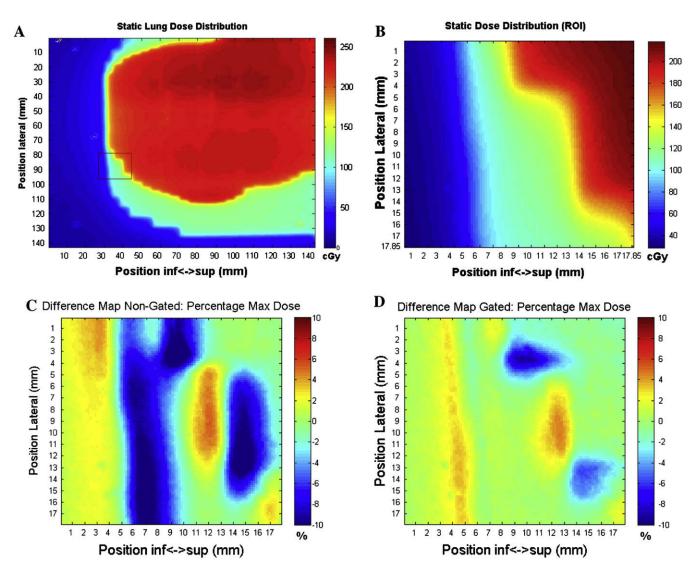

Fig. 5. Dose difference maps. Films irradiated in presence of clinically relevant motion subtracted from the static reference case. (A) Entire dose profile. (B) High-gradient region of interest as denoted by box in Fig. a. (C,D) Normalized difference maps calculated to show over- and underdosing as percentage of maximal dose. Red and blue regions indicate over- and underdosing, respectively. Gating reduced spread and magnitude of dose mismatch occurring in presence of motion.

software implementation of the gating decision unit, as well as to the finite integration times of the transponders (26 ms). The latency associated with enacting a beam hold or re-establishing treatment by way of the linear accelerator was relatively small, approximately 17 ms (27). Given the experimental setup, this value was incorporated into the total latency values reported for the spatial gating system. The update rates and latencies of the system were comparable to the optical-based (28) and fluoroscopy-based (15) gating systems reported previously.

Gating: clinical dosimetry

Dosimetric films were used to determine the dose profile from one fraction of treatment. One baseline run with no motion was used to generate a static film. This film was used as the ideal dose distribution in the absence of patient motion. The static film was compared with the films irradiated using the same treatment plan delivered both with and without gating in the presence of motion. Using beam gating, better dose localization was observed, and the film results showed better correlation with the static dose distribution (Fig. 5). The effects of gating were most evident in the regions of a high-dose gradient, because the nongated case effectively "blurs" the dose over the region that passes through the isocenter during respiratory motion. Difference maps have shown that the dose blurring found in the nongated dynamic case is significantly reduced when the gating solution is implemented (Fig. 5). Dosimetric analysis was performed to quantify the level of over- and underdosing. For the no-intervention case, 32.1% of the points failed to be within ±10 cGy from the ideal dose and 8.6% failed for ±20 cGy. For gating, 3.4% failed for ±10 cGy and 0.0% failed to be within ±20 cGy.

Gamma analysis was performed on the nongated and gated films. Although no points failed a 3-mm/3% test, 8.3% of the points in the nongated film failed at 1.5 mm/1.5% compared with 0% of the points in the gated film (Fig. 6).

It is evident from multiple line profiles that gating produces an increase in the achievable dose gradients (Fig. 7). This increase in dose gradients has clinical implications, which have been addressed in the "Discussion" section.

Even when considering the small gating window used for the present study, the duty cycle was 47% and 49%, respectively, for each of the two lung trajectories. This shows that for most cases the increase in treatment time was small compared with the time spent initially aligning the patient and moving the gantry to the various beam angles. This will not be the case for instances of drastic motion or when the target leaves the gating volume for an extended period.

DISCUSSION

Gating is a widely used technique for dose localization. One of the limiting factors in the effectiveness of gating is that most implementations use external markers to predict the internal movement of tumors. Although studies have shown a correlation between external and internal motion, variations of about 1 cm have been found between internal fiducial motion and external markers (10, 13). Thus, it is important to implement a solution for determining the precise location of the internal anatomy without exposing the patient to an additional imaging dose throughout the treatment course.

It has been shown that large latencies can produce a phase mismatch between beam gating and the tumor position (28). For the initial studies shown in the present report, a software-based decision-making setup was implemented. For clinical implementation, a hardware-based solution would offer lower latencies. The latencies associated with our system are as good as or better than alternative options. For instance, fluoroscopic and optical gating systems have claimed latencies of ~90 ms (15) and 170 ms (cite 28) ms, respectively. Note, the low latencies associated with our setup demonstrated a measurable dosimetric difference without the use of predictive algorithms (29). This internal tracking implementation
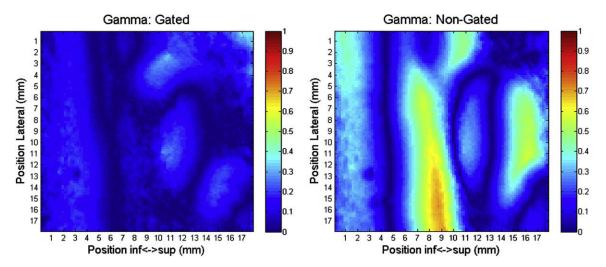

Fig. 6. Gamma (3-mm/3%) maps for gated and nongated cases for region of interest denoted in Fig. 5.
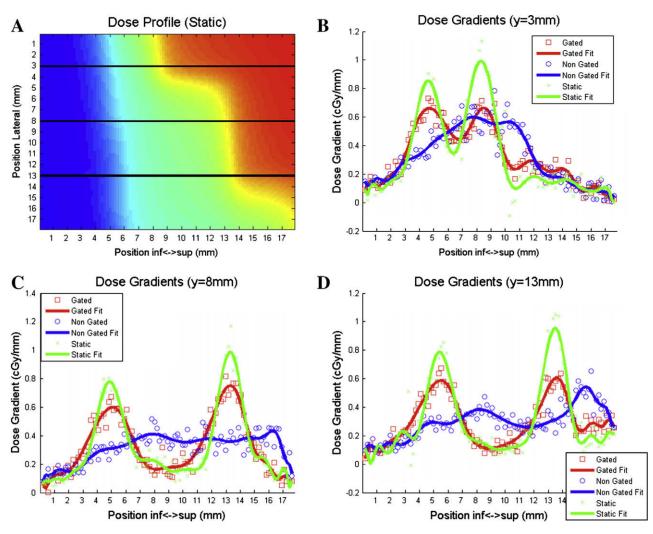
Fig. 7. (A) Static dose profile. Gating reduced dose blurring and improved dose gradients compared with no intervention. (B–D) Dose gradients of line profiles analyzed for lines at y = 3 mm, 8 mm, and 13 mm. Raw data plotted with polynomial fit overlaid. Gating improved dose gradients to match delivery in absence of motion.

can be incorporated with any linear accelerator in a standard-size vault.

In clinical implementation, the exact dimensions of the 3D gating volume will likely vary from patient to patient. The 3D volume would be chosen according to a number of factors: the relationship and level of correlation between the transponder and the tumor as evidenced by respiratory-correlated imaging, the proximity to normal structures, the amount of target motion, and the desired efficiency of the treatment. The number of implanted transponders will have an adverse affect on the update rate of the system. The use of a single transponder increases the acquisition frequency for the spatial position information, but at the expense of the rotational information obtained by using multiple transponders. Studies are needed to determine the cost/benefit ratio from acquiring spatial information from multiple transponders compared with the additional latency associated with multiple transponder readings. For instance, in one potential clinical implementation, multiple transponders could be used during the patient setup process, but a single transponder could be localized for gating throughout the treatment course.

Work is needed to ensure that implantation in the lung is safe. Pneumothorax is a typical complication with percutaneous implantation of a fiducial marker in the lung. Although bronchoscopic implants have lower pneumothorax rates (1.8%) (30) than implants done percutaneously (33%) (31), additional work is needed to ensure the system is safe for patient use. Research to develop a bronchoscopic implantation technique for electromagnetic transponders is promising (32).

Additionally, the implanted electromagnetic transponders have been shown to be stable in the prostate. Targeting of a lung tumor might be more challenging, because the transponders will not likely have a fixed relationship to the lung tumor. The incorporation of the uncertainty will affect the size of a gating window. Work on a modified transponder design with stability features has shown good fixation to lung tissue (32).

If left unchecked, breathing motion prevents high-dose gradient regions in which the delivered dose to the surrounding healthy tissue decays rapidly. High-dose gradients are necessary for dose escalation to tumor sites while ensuring that the surrounding critical structures do not receive a substantial dose. As noted in Fig. 7, the dose gradients achieved using the gating solution were larger than those achieved with no intervention in the presence of motion.

CONCLUSION

An electromagnetic tracking system has been successfully interfaced with a linear accelerator gating system. The latencies measured were comparable to those of other real-time radiotherapy systems, and film experiments using realistic lung trajectories showed that gating provides significant dosimetric improvements.

REFERENCES

1. Langen KM, Jones DT. Organ motion and its management. *Int J Radiat Oncol Biol Phys* 2001;50:265–278.
2. Ramsey CR, Cordrey IL, Oliver AL. A comparison of beam characteristics for gated and nongated clinical x-ray beams. *Med Phys* 1999;26:2086–2091.
3. Pan T, Lee TY, Rietzel E, *et al*. 4D-CT imaging of a volume influenced by respiratory motion on multi-slice CT. *Med Phys* 2004;31:333–340.
4. Shirato H, Shimizu S, Kunieda T, *et al*. Physical aspects of a real-time tumor-tracking system for gated radiotherapy. *Int J Radiat Oncol Biol Phys* 2000;48:1187–1195.
5. Margeras G, Yorke E, Rosenzweig K. Initial clinical evaluation of a respiratory gating radiotherapy system. Proceedings of the 22nd annual EMBS International Conference, July 23–28, 2000, Chicago, IL.
6. Kini VR, Vedam SS, Keall PJ, *et al*. Patient training in respiratory-gated radiotherapy. *Med Dosim* 2003;28:7–11.
7. Kubo HD, Len PM, Minohara S, *et al*. Breathing-synchronized radiotherapy program at the University of California Davis Cancer Center. *Med Phys* 2000;27:346–353.
8. Berson AM, Emery R, Rodriguez L, *et al*. Clinical experience using respiratory gated radiation therapy: Comparison of free-breathing and breath-hold techniques. *Int J Radiat Oncol Biol Phys* 2004;60:419–426.
9. Kubo HD, Hill BC. Respiration gated radiotherapy treatment: A technical study. *Phys Med Biol* 1996;41:83–91.
10. Gierga DP, Brewer J, Sharp GC, *et al*. The correlation between internal and external markers for abdominal tumors: Implications for respiratory gating. *Int J Radiat Oncol Biol Phys* 2005;62:1551–1558.
11. Margeras GS, Yorke E. Deep inspiration breath hold and respiratory gating strategies for reducing organ motion in radiation treatment. *Semin Radiat Oncol* 2004;14:65–75.
12. Koch N, Liu HH, Starkschall G, *et al*. Evaluation of internal lung motion for respiratory-gated radiotherapy using MRI: Part I—Correlating internal lung motion with skin fiducial motion. *Int J Radiat Oncol Biol Phys* 2004;60:1459–1472.
13. Berbeco RI, Nishioka S, Shirato H, *et al*. Residual motion of lung tumours in gated radiotherapy with external respiratory surrogates. *Phys Med Biol* 2005;50:3655–3667.
14. Ozhasoglu C, Murphy MJ. Issues in respiratory motion compensation during external-beam radiotherapy. *Int J Radiat Oncol Biol Phys* 2002;52:1389–1399.
15. Shimizu S, Shirato H, Ogura S, *et al*. Detection of lung tumor movement in real-time tumor-tracking radiotherapy. *Int J Radiat Oncol Biol Phys* 2001;51:304–310.
16. Shirato H, Oita M, Fujita K, *et al*. Feasibility of synchronization of real-time tumor-tracking radiotherapy and intensity-modulated radiotherapy from viewpoint of excessive dose from fluoroscopy. *Int J Radiat Oncol Biol Phys* 2004;60:335–341.

17. Seppenwoolde Y, Berbeco RI, Nishioka S, *et al*. Accuracy of tumor motion compensation algorithm from a robotic respiratory tracking system: A simulation study. *Med Phys* 2007;34:2774–2784.
18. Murphy MJ, Balter J, Balter S, *et al*. The management of imaging dose during image-guided radiotherapy: Report of the AAPM Task Group 75. *Med Phys* 2007;34:4041–4063.
19. Berbeco RI, Jiang SB, Sharp GC, *et al*. Integrated radiotherapy imaging system (IRIS): Design considerations of tumour tracking with linac gantry-mounted diagnostic x-ray systems with flat-panel detectors. *Phys Med Biol* 2004;49:243–255.
20. Luo W, Yoo S, Wu J, *et al*. Effect of MV scatter on kV image quality during simultaneous kV-MV imaging. *Int J Radiat Oncol Biol Phys* 2007;69:S671.
21. Balter JM, Wright JN, Newell LJ, *et al*. Accuracy of a wireless localization system for radiotherapy. *Int J Radiat Oncol Biol Phys* 2005;61:933–937.
22. Santanam L, Malinowski K, Hubenshmidt J, *et al*. Fiducial-based translational localization accuracy of electromagnetic tracking system and on-board kilovoltage imaging system. *Int J Radiat Oncol Biol Phys* 2008;70:892–899.
23. Willoughby TR, Kupelian PA, Pouliot J, *et al*. Target localization and real-time tracking using the Calypso 4D localization system in patients with localized prostate cancer. *Int J Radiat Oncol Biol Phys* 2006;65:528–534.
24. Parikh P, Hubenschmidt J, Dimmer S, *et al*. 4D verification of real-time accuracy of the Calypso system with lung cancer patient trajectory data. *Int J Radiat Oncol Biol Phys* 2005;63:S26–S27.
25. Malinowski K, Lechleiter K, Hubenschmidt J, *et al*. Use of the 4D phantom to test real-time targeted radiation therapy device accuracy. *Med Phys* 2007;34:2611.
26. Low DA, Parikh PJ, Lu W, *et al*. Novel breathing motion model for radiotherapy. *Int J Radiat Oncol Biol Phys* 2005;63:921–929.
27. Hanna G, Wang Z, Yin F. Time-delay measurement of a Varian real-time position management system. *Med Phys* 2006;33:2145.
28. Jin J, Yin F. Time delay measurement for linac based treatment delivery in synchronized respiratory gating radiotherapy. *Med Phys* 2005;32:1293–1296.
29. Sharp GC, Jiang SB, Shimizu S, *et al*. Prediction of respiratory tumour motion for real-time image-guided radiotherapy. *Phys Med Biol* 2004;49:425–440.
30. Imura M, Yamazaki K, Shirato H, *et al*. Insertion and fixation of fiducial markers for setup and tracking of lung tumors in radiotherapy. *Int J Radiat Oncol Biol Phys* 2005;63:1442–1447.
31. Whyte RI, Crownover R, Murphy MJ, *et al*. Stereotactic radiosurgery for lung tumors: Preliminary report of a phase I trial. *Ann Thorac Surg* 2003;75:1097–1101.
32. Mayse ML, Smith RL, Park M. Development of a non-migrating electromagnetic transponder system for lung tumor tracking. *Int J Radiat Oncol Biol Phys* 2008;72(Suppl.):S430.